



# On the evolution and physiology of cable bacteria

Kasper U. Kjeldsen<sup>a,1</sup>, Lars Schreiber<sup>a,b,1</sup>, Casper A. Thorup<sup>a,c</sup>, Thomas Boesen<sup>c,d</sup>, Jesper T. Bjerg<sup>a,c</sup>, Tingting Yang<sup>a,e</sup>, Morten S. Dueholm<sup>f</sup>, Steffen Larsen<sup>a</sup>, Nils Risgaard-Petersen<sup>a,c</sup>, Marta Nierychlo<sup>f</sup>, Markus Schmid<sup>g</sup>, Andreas Bøggild<sup>d</sup>, Jack van de Vossenberg<sup>h</sup>, Jeanine S. Geelhoed<sup>i</sup>, Filip J. R. Meysman<sup>i,j</sup>, Michael Wagner<sup>f,g</sup>, Per H. Nielsen<sup>f</sup>, Lars Peter Nielsen<sup>a,c</sup>, and Andreas Schramm<sup>a,c,2</sup>

<sup>a</sup>Section for Microbiology & Center for Geomicrobiology, Department of Bioscience, Aarhus University, 8000 Aarhus, Denmark; <sup>b</sup>Energy, Mining and Environment Research Centre, National Research Council Canada, Montreal, QC H4P 2R2, Canada; <sup>c</sup>Center for Electromicrobiology, Aarhus University, 8000 Aarhus, Denmark; <sup>d</sup>Interdisciplinary Nanoscience Center & Department of Molecular Biology and Genetics, Aarhus University, 8000 Aarhus, Denmark; <sup>e</sup>Department of Biological Oceanography, Leibniz Institute for Baltic Sea Research, Warnemünde (IOW), 18119 Rostock, Germany; <sup>f</sup>Center for Microbial Communities, Department of Chemistry and Bioscience, Aalborg University, 9220 Aalborg, Denmark; <sup>g</sup>Centre for Microbiology and Environmental Systems Science, University of Vienna, 1090 Vienna, Austria; <sup>h</sup>Environmental Engineering and Water Technology (EEWT) Department, IHE Delft Institute for Water Education, 2611 AX Delft, The Netherlands; <sup>i</sup>Department of Biology, University of Antwerp, 2610 Wilrijk (Antwerpen), Belgium; and <sup>j</sup>Department of Biotechnology, Delft University of Technology, 2629 HZ Delft, The Netherlands

Edited by Edward F. DeLong, University of Hawaii at Manoa, Honolulu, HI, and approved July 23, 2019 (received for review February 28, 2019)

**Cable bacteria of the family Desulfobulbaceae form centimeter-long filaments comprising thousands of cells. They occur worldwide in the surface of aquatic sediments, where they connect sulfide oxidation with oxygen or nitrate reduction via long-distance electron transport. In the absence of pure cultures, we used single-filament genomics and metagenomics to retrieve draft genomes of 3 marine *Candidatus* *Electrothrix* and 1 freshwater *Ca. Electronema* species. These genomes contain >50% unknown genes but still share their core genomic makeup with sulfate-reducing and sulfur-disproportionating Desulfobulbaceae, with few core genes lost and 212 unique genes (from 197 gene families) conserved among cable bacteria. Last common ancestor analysis indicates gene divergence and lateral gene transfer as equally important origins of these unique genes. With support from metaproteomics of a *Ca. Electronema* enrichment, the genomes suggest that cable bacteria oxidize sulfide by reversing the canonical sulfate reduction pathway and fix CO<sub>2</sub> using the Wood-Ljungdahl pathway. Cable bacteria show limited organotrophic potential, may assimilate smaller organic acids and alcohols, fix N<sub>2</sub>, and synthesize polyphosphates and polyglucose as storage compounds; several of these traits were confirmed by cell-level experimental analyses. We propose a model for electron flow from sulfide to oxygen that involves periplasmic cytochromes, yet-unidentified conductive periplasmic fibers, and periplasmic oxygen reduction. This model proposes that an active cable bacterium gains energy in the anodic, sulfide-oxidizing cells, whereas cells in the oxic zone flare off electrons through intense cathodic oxygen respiration without energy conservation; this peculiar form of multicellularity seems unparalleled in the microbial world.**

electromicrobiology | microbial genome | cable bacteria | microbial evolution | microbial physiology

**C**able bacteria are multicellular, filamentous bacteria (1, 2) found worldwide in marine and freshwater sediments (3–5). They facilitate long-distance electron transport (LDET) over centimeter distances (6), thereby coupling the oxidation of sulfide (H<sub>2</sub>S) in deeper sediment layers with the reduction of O<sub>2</sub> or nitrate near the sediment–water interface (Fig. 1A) (1, 7). Phylogenetically, cable bacteria belong to the delta-proteobacterial family Desulfobulbaceae (1), which otherwise is known to contain sulfate-reducing or sulfur-disproportionating species but not canonical, aerobic sulfide oxidizers (8). Based on 16S rRNA gene sequence phylogeny, cable bacteria form a monophyletic sister group to the genus *Desulfobulbus* (9). Currently, the cable bacteria clade consists of the genera “*Candidatus* *Electrothrix*” and “*Candidatus* *Electronema*,” with 6 described candidate species (9); so far, none of them has been isolated into pure culture.

Cable bacteria can dominate benthic microbial communities (3, 10), and the cable bacteria-associated electrogenic sulfur oxidation (e-SOX) can account for the larger part of a sediment’s

oxygen consumption (2, 3, 11). The metabolic activity of cable bacteria has distinct effects on sediment biogeochemistry (11–13), especially on the cycling of sulfur, iron, phosphorus, and nitrogen, with implications for eutrophication and habitability of sediments (14–16). Notably, cable bacteria induce the formation of a 1- to 4-cm-deep suboxic zone devoid of O<sub>2</sub> and H<sub>2</sub>S and a pronounced pH peak in the oxic zone, consistent with the consumption of protons during O<sub>2</sub> reduction to water (1, 11, 12).

Based on these biogeochemical observations, it has been suggested that cells within an individual cable bacterium filament can display 2 types of metabolism: “anodic” cells oxidize sulfide in the anoxic zone, and the resulting electrons are transported along the longitudinal axis of the filament to the oxic zone, where “cathodic” cells use the electrons to reduce oxygen (Fig. 1A) (1, 17). LDET along living, individual cable bacteria filaments has

## Significance

**Cable bacteria are globally occurring multicellular filamentous bacteria that are electrically conductive: they transfer electrons from sulfide oxidation at one end over centimeter distances to oxygen reduction at the other end. Unlike any other organism known, cable bacteria thus split their central energy-conserving redox reaction into 2 half-reactions that occur in different cells as far as several centimeters apart. Before this study, the molecular foundation, evolutionary origin, and genomic basis of this unique metabolism were unknown. Here we reconstructed 5 genomes from single filaments and 1 from a cable bacterium enrichment culture to shed light on the evolution and physiology of cable bacteria; and, together with proteomic and experimental data, we propose a metabolic model of how cable bacteria work.**

Author contributions: K.U.K., L.S., and A.S. designed research; K.U.K., L.S., C.A.T., T.B., J.T.B., T.Y., M.S.D., S.L., N.R.-P., M.N., M.S., A.B., L.P.N., and A.S. performed research; M.W., P.H.N., and A.S. contributed new reagents/analytic tools; K.U.K., L.S., C.A.T., T.B., J.T.B., T.Y., M.S.D., A.B., J.v.d.V., J.S.G., F.J.R.M., M.W., and A.S. analyzed data; and K.U.K., L.S., F.J.R.M., and A.S. wrote the paper.

The authors declare no conflict of interest.

This article is a PNAS Direct Submission.

Published under the PNAS license.

Data deposition: All genomic data analyzed in this manuscript have been submitted to GenBank (<https://www.ncbi.nlm.nih.gov/genbank/>) under the Bioproject IDs PRJNA187269 (MCF), PRJNA389779 (GS), and PRJNA278504 (genomes A1, A2, A3, and A5). The mass spectrometry proteomics data have been deposited to the ProteomeXchange Consortium (<http://www.proteomexchange.org>) via the PRIDE partner repository with the dataset identifier PXD012775.

See Commentary on page 18759.

<sup>1</sup>K.U.K. and L.S. contributed equally to this work.

<sup>2</sup>To whom correspondence may be addressed. Email: andreas.schramm@bios.au.dk.

This article contains supporting information online at [www.pnas.org/lookup/suppl/doi:10.1073/pnas.1903514116/-DCSupplemental](https://www.pnas.org/lookup/suppl/doi:10.1073/pnas.1903514116/-DCSupplemental).

Published online August 19, 2019.

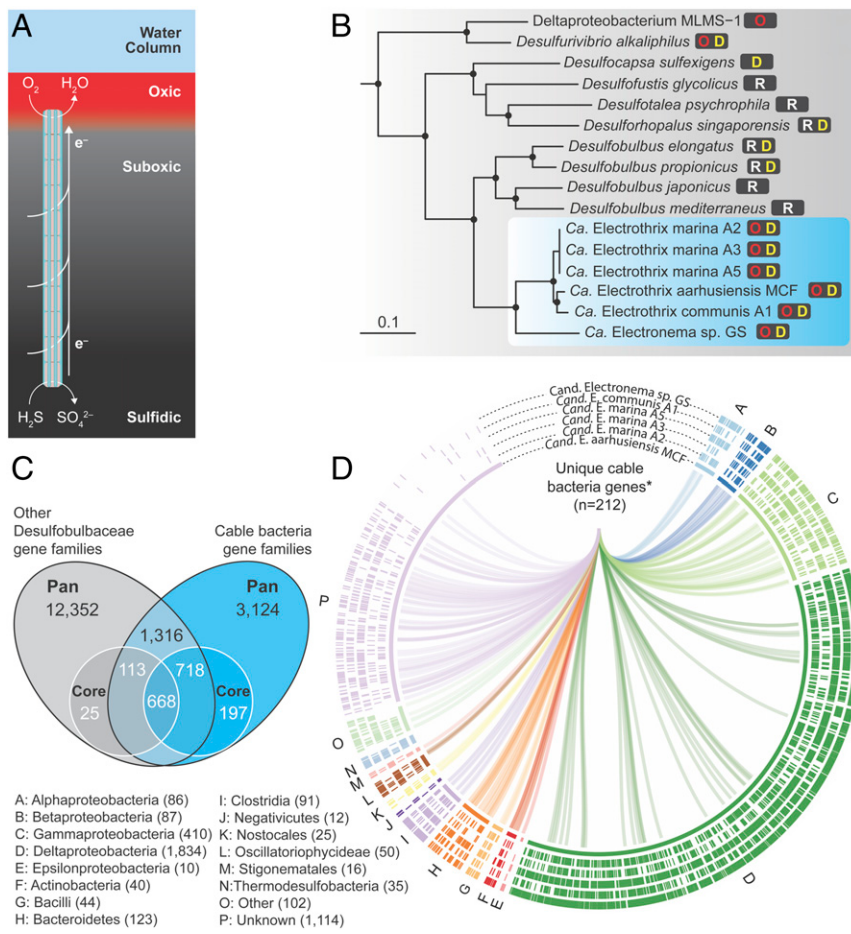


**Fig. 1.** (A) Conceptual model of electrogenic sulfur oxidation in aquatic sediments by cable bacteria. Anodic cells oxidize sulfide in the anoxic zone deeper in the sediment, and the electrons derived from sulfide are transported through the cable bacteria into the oxic zone, where cathodic cells use them to reduce oxygen. (B) Phylogeny of the Desulfobulbaceae inferred by maximum likelihood analysis based on the concatenated amino acid sequence of 31 single-copy genes conserved within the Desulfobulbaceae. Cable bacteria form a monophyletic group (blue box). Full circles at tree nodes indicate 100% bootstrap support. The scale bar represents 10% estimated sequence changes. Colored letters indicate the primary energy metabolism of the associated species: O (red), sulfide oxidation; R (black), sulfate reduction, D (yellow), sulfur disproportionation. (C) Comparative analysis between genomes of cable bacteria and other Desulfobulbaceae. For core gene families of cable bacteria, simultaneous presence in *Ca. E. aarhusiensis* MCF and *Ca. Electronema* sp. GS was interpreted as present in the whole group. (D) Comparison and origin of genes of cable bacteria genomes. The inner ring shows the concatenated genes of the genome of *Ca. E. aarhusiensis* MCF grouped by last common ancestor (LCA; predicted by MEGAN with default settings; only LCA groups with at least 10 assigned genes were considered). The total numbers of genes for each LCA group are shown in brackets. Similar genes ( $\geq 75\%$  nucleotide identity; BLASTN) in the draft genomes of other cable bacteria are indicated in the outer circles. \*The 212 unique genes, i.e., present in cable bacteria but not in other previously published Desulfobulbaceae genomes (identified by bidirectional best BLAST hit via ITEP and representing 197 gene families), are indicated with inner-circle links.

recently been demonstrated using resonance Raman microscopy (18); other metabolic traits have only been indirectly inferred from the disappearance of substrates or the appearance of metabolites in the sediment environment. A consistent model for cable bacteria metabolism and intra- and intercellular electron transport is currently lacking, and the evolutionary origin of this unique lifestyle remains unclear. Likewise, neither the mechanism of LDET nor the underlying biological structures have been identified; the best candidates are continuous periplasmic fibers of unknown composition that run along the entire filament length and show charge storage capacity (1, 19, 20).

Here we reconstruct cable bacteria draft genomes from individual *Ca. Electrothrix* filaments and a *Ca. Electronema* enrichment, identify highly expressed proteins by metaproteomic analysis of a *Ca. Electronema* sediment enrichment, and visualize selected traits in individual filaments. The goal of this proteogenomic approach was to gain insight into the evolution and physiology of cable bacteria and to reconstruct a consistent model for the metabolism of this unique life form.

## Results and Discussion

**Cable Bacteria Largely Feature the Core Genome of Desulfobulbaceae and Contain Many Unique Genes.** We assembled 5 genomes of *Ca. Electrothrix* from 6 individual filaments, picked from marine sediment, and 1 genome of *Ca. Electronema* from a metagenome of a freshwater enrichment culture (see *SI Appendix* for details). Phylogenetic analysis of 31 concatenated, conserved single-copy genes placed the cable bacteria as a monophyletic sister group to the genus *Desulfobulbus* within the delta-proteobacterial family Desulfobulbaceae (Fig. 1B), thus confirming previous 16S rRNA-based analyses (1, 9). The genomes were 21 to 93% complete, with

a GC content of 47.5 to 51.9% and an estimated genome size of 2.7 to 4.0 Mbp (*SI Appendix*, Table S1), well within the range of the Desulfobulbaceae family (*SI Appendix*, Table S2). Based on their average nucleotide identities (ANIs), the 6 genomes represent 4 cable bacteria species (*SI Appendix*, Table S3), of which *Ca. Electrothrix aarhusiensis* MCF and *Ca. Electronema* sp. GS showed the most complete genomes (both 93%). Therefore, they form the basis of this study, whereas the remaining genomes of the species *Ca. Electrothrix communis* and *Ca. Electrothrix marina* were used as complementary information to help identify general trends.

The Desulfobulbaceae contain primarily single-celled sulfate-reducing bacteria, but (compared with other delta-proteobacterial families) also a large fraction of sulfur disproportionators, and some species can even grow by sulfide oxidation (Fig. 1B) (8). This somewhat unusual lineage might thus have been well prepared for the evolutionary innovations that gave rise to cable bacteria. In fact, the morphologically and metabolically distinct cable bacteria still largely feature the core genomic makeup of the Desulfobulbaceae, including an almost complete canonical dissimilatory sulfate reduction (DSR) pathway (as detailed later). Only 25 of the 806 core gene families of the Desulfobulbaceae were not detected in any of the cable bacteria genomes (Fig. 1C and D). Core gene families missing in cable bacteria include gene families that encode flagella, the glycolytic enzyme enolase, subunits DsrOP of the DsrKMJOP complex (21), and the original NADH-quinone oxidoreductase (Nuo) enzyme complex, which has apparently been replaced with a xenolog by lateral gene transfer (*SI Appendix*, Table S4).

A comparison of the cable bacteria genomes versus other Desulfobulbaceae using the Clusters of Orthologous Groups (COG) revealed that the functional categories “energy production

and conversion,” “amino acid transport and metabolism,” and “carbohydrate transport and metabolism” were underrepresented in cable bacteria genomes (*SI Appendix*, Fig. S1A). This is a first indication of a limited organotrophic catabolic potential (as discussed later). Furthermore, and consistent with their unique lifestyle, a large fraction (37 to 66%) of cable bacteria genes could not be assigned to a COG category (*SI Appendix*, Fig. S1A), and many gene families were unique and not found in other Desulfobulbaceae. In “*Ca. E. aarhusiensis* MCF,” a total of 1,721 gene families, representing approximately 44% of its total gene families, were not present in other Desulfobulbaceae or highly divergent from their homologs. Of these, 385 were also detected in at least one of the other, more incomplete *Ca. Electrothrix* genomes. Across the *Ca. Electrothrix*/*Electronema* genus boundary, 197 gene families (representing 212 individual genes) were unique and conserved for the cable bacteria lineage (Fig. 1C and D and *Dataset S1*). Last common ancestor (LCA) analysis (Fig. 1D) predicted that approximately half of these cable bacteria-specific genes originated from Deltaproteobacteria (21.7%) or Gammaproteobacteria (28.8%), including many from the sulfur-oxidizing orders Chromatiales and Thiotrichales (22–24). Approximately 20% of the cable bacteria-specific genes could not be assigned to an ancestral lineage, indicating an origin from a genetically undescribed donor lineage or that they arose from evolutionary innovation. The functional role of these cable bacteria-specific gene families could not be determined, as almost half of them encode hypothetical proteins and 71% could not be assigned a COG category (*SI Appendix*, Fig. S1B). Remarkably, however, approximately one third of them has a predicted extracytoplasmic or membrane localization (*SI Appendix*, Fig. S1B), suggesting major innovations in the cell envelope, which is consistent with the conspicuous ultrastructure of the cable bacterium cell envelope (20).

The high number of conserved Desulfobulbaceae genes as well as unique cable bacteria genes (Fig. 1C and D), together with an average Desulfobulbaceae genome size (*SI Appendix*, Tables S1 and S2), suggests that the divergence of the cable bacteria clade (Fig. 1B) and the evolution of the unique filamentous “electrogenic lifestyle” of its members were driven by neither massive gene loss nor major genome expansion. Rather, substantial horizontal gene transfer in combination with the moderate replacement and divergence of ancestral genes was key for the evolution of cable bacteria. This could imply that electric conduction along filaments may also have evolved in other phylogenetic lineages, as indicated by putative LDET in a filamentous groundwater Desulfobulbaceae species distinct from the *Ca. Electrothrix*/*Electronema* clade (25), or the possibly electric signal transduction in the filamentous cyanobacterium *Phormidium uncinatum* (26).

**Cable Bacteria Likely Oxidize Sulfide by Reversal of the Canonical Sulfate Reduction Pathway.** The current conceptual model for cable bacteria metabolism, consistent with the large body of geochemical data (as reviewed in ref. 17), is that anodic sulfide oxidation in anoxic cells is coupled via LDET by continuous periplasmic fibers over thousands of cells to cathodic oxygen reduction in oxic cells (Fig. 1A). To assess this hypothesis and to shed further light on the physiology of cable bacteria, we combined the genome dataset with metaproteomics for the *Ca. Electronema* sp. GS enrichment culture. The proteomic data covered 313 of the 2,649 predicted genes of *Ca. Electronema* sp. GS, with a few genes approximately 10-fold higher expressed than the rest (Fig. 2 and *Dataset S2*). Cable bacteria lack genes diagnostic for sulfide-oxidizing bacteria, i.e., genes encoding the Sox pathway, reverse-type dissimilatory sulfite reductase (rDSR), or flavocytochrome C sulfide dehydrogenase (27). In contrast, and consistent with their evolutionary descent from sulfate-reducing Desulfobulbaceae, cable bacteria encode all key genes of the canonical sulfate reduction (DSR) pathway (21, 28) (Fig. 3 and

*Dataset S2*), and many of them were highly expressed in *Ca. Electronema* sp. GS (Fig. 2 and *Dataset S2*). We propose that cable bacteria reverse this pathway for sulfide oxidation and, in this respect, resemble their close relative *Desulfurivibrio alkaliphilus* (Fig. 1B), which grows by nitrate-dependent sulfide oxidation and sulfur disproportionation (29). In *D. alkaliphilus*, sulfide is initially oxidized to elemental sulfur, which is then disproportionated or oxidized to sulfate (29, 30). Such a 2-step process has also been concluded from physiological studies of sulfate reducers capable of aerobic sulfide oxidation (31). The best candidate enzyme for the first step in *D. alkaliphilus* is a type I sulfide:quinone oxidoreductase (SQR) (29), whereas, in cable bacteria, a type III SQR is present and expressed (*SI Appendix*, Fig. S2 and *SI Discussion*). Sulfur produced by SQR in the periplasm can react chemically with sulfide to form dissolved polysulfide (Fig. 3) or may be transported into the cytoplasm. Cable bacteria encode a membrane-anchored polysulfide reductase (PSR), which was expressed in *Ca. Electronema* sp. GS (Fig. 3) and can reduce polysulfide to sulfide with electrons from the quinone pool in the cytoplasmic membrane. Unlike SQR, PSR may conserve energy by proton translocation (32) while

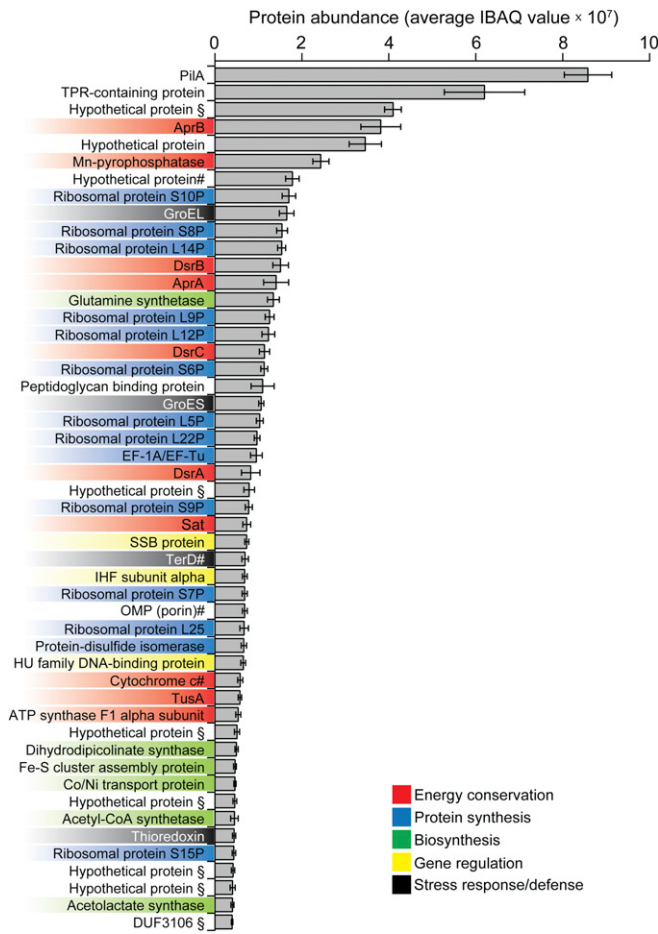


**Fig. 2.** Top 50 most abundant proteins detected in the proteome of *Ca. Electronema* sp. GS. Protein abundances were quantified and expressed as intensity-based absolute abundance (IBAQ); average values  $\pm$ SD of 6 individual analyses are shown. *Dataset S2* provides details including locus tags and abbreviation of protein names. The inferred functional category of proteins is indicated by color. #Protein encoded by a gene uniquely conserved in cable bacteria relative to other Desulfobulbaceae (see *Dataset S1* for details). §Protein encoded by a gene unique to *Ca. Electronema* sp. GS relative to other cable bacteria.

balancing the reduced quinone pool. Sulfur disproportionation, by combining PSR activity with sulfur oxidation to sulfate, may allow energy conservation in cable bacterial cells when disconnected from their external electron acceptors oxygen or nitrate.

In the second step, sulfur formed by the activity of SQR could be oxidized to sulfate by a reversal of the cytoplasmic DSR pathway (Fig. 3). The transport mechanism of elemental sulfur across the cytoplasmic membrane is generally poorly resolved, but may involve the membrane protein YeeE, a cytoplasmic

rhodanese, and the sulfur transferases TusA and DsrEFH (33, 34). Homologs of YeeE, rhodanese, and TusA are encoded in the cable bacteria genomes (Fig. 3 and *Dataset S3*), and the rhodanese and TusA homologs were expressed in *Ca. Electronema* sp. GS (Fig. 3 and *Dataset S2*). In contrast, DsrEFH is not encoded in cable bacteria genomes (*SI Appendix, SI Discussion*). According to our model, reduced sulfur from TusA, but possibly also directly from sulfide, reacts with DsrC to form DsrC-trisulfide (DCT). DCT is then oxidized by the dissimilatory

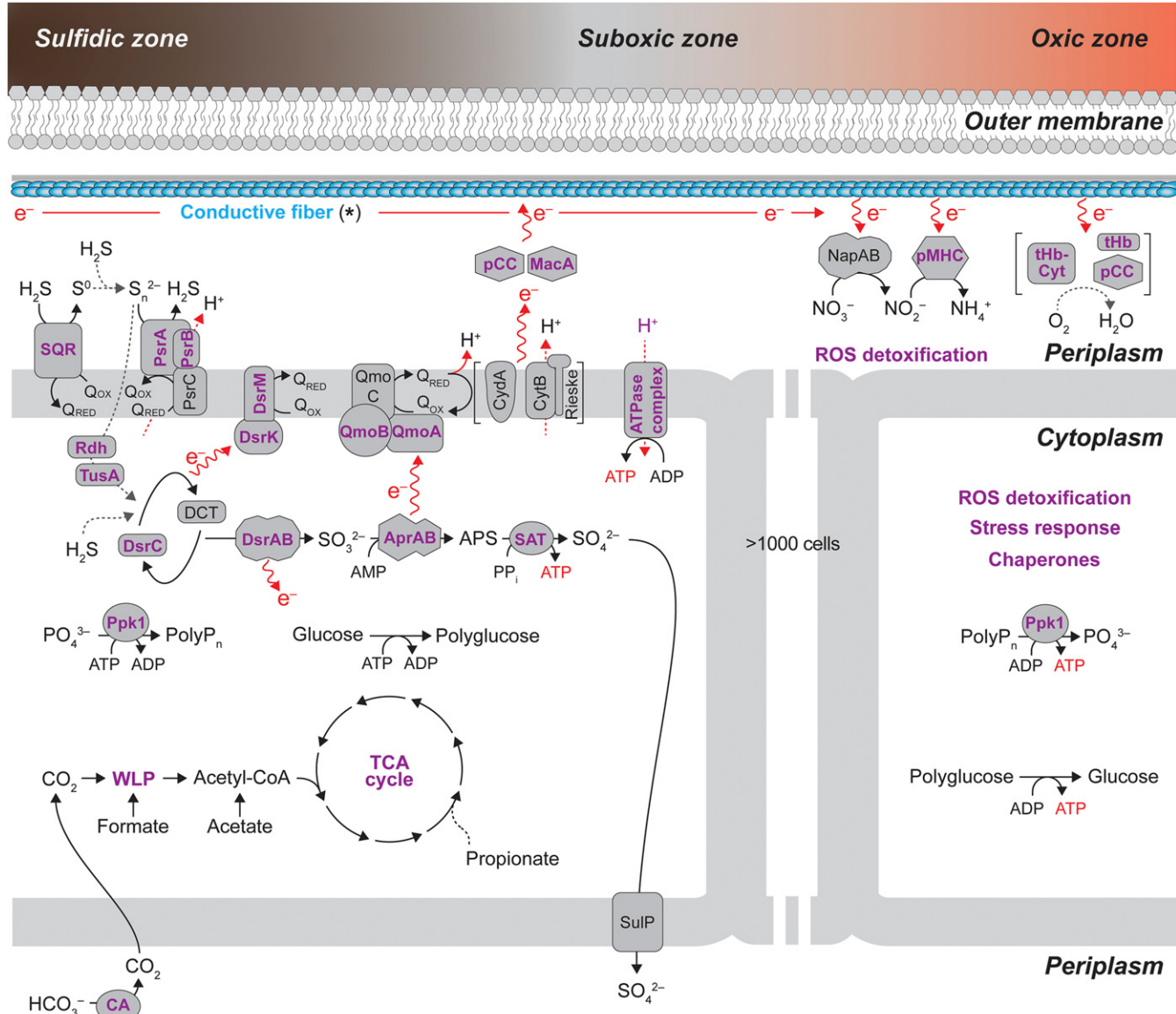


**Fig. 3.** Genome-based metabolic model for cable bacteria with emphasis on electron flow and energy conservation during oxygen and nitrate-dependent sulfide oxidation. One anodic cell (Left) and one cathodic cell (Right) are shown. Electron transport between anodic and cathodic cells is indicated by red arrows. Gray dotted arrows indicate putative reactions with an unclear enzymatic foundation. Proteins detected in the proteome of *Ca. Electronema* sp. GS are indicated in purple boldface. Only marine cable bacteria possess the genetic potential for propionate assimilation. Apr, Adenosine phosphosulfate reductase; CA, carbonic anhydrase; CydA, membrane-bound cytochrome bd quinol oxidase-subunit A; CytB, cytochrome bc complex-subunit B; DCT, DsrC-trisulfide; Dsr, dissimilatory bisulfite reductase; MacA, cytochrome c peroxidase; Nap, periplasmic nitrate reductase; pCC, periplasmic cytochrome C; pMHC, periplasmic multiheme cytochrome (nitrite reductase); PolyP, polyphosphate; Ppk, polyphosphate kinase; Psr, polysulfide reductase; Q<sub>OX/RED</sub>, quinone (oxidized or reduced); Qmo, quinone-interacting membrane-bound oxidoreductase complex; Rdh, rhodanese; Rieske, Rieske Fe-S domain protein; ROS, reactive oxygen species; Sat, ATP sulfurylase; SQR, sulfide:quinone oxidoreductase; TCA, tricarboxylic acid cycle; tHb, truncated hemoglobin; tHb-Cyt, truncated hemoglobin-cytochrome domain fusion protein; TusA, sulfur transferase; WLP, Wood-Ljungdahl pathway. Periplasmic enzymes include superoxide reductase and hydrogen peroxide reductase; cytoplasmic enzymes include catalase. Asterisk indicates an unknown molecular structure of the conductive fiber. Further details are provided in the main text and *SI Appendix, SI Discussion*.

bisulfite reductase DsrAB to release sulfite and DsrC (28). Sulfite is further oxidized to sulfate by adenosine-5-phosphosulfate reductase (AprAB) and sulfate adenyltransferase (Sat), generating ATP by substrate level phosphorylation in the process (35). Finally, sulfate is transported out of the cell by SulP, which is considered a common sulfate transporter in SRM (36).

Our genomic data suggest that electrons released by the oxidation of reduced DsrC and of sulfite are transferred to the quinone pool in the cytoplasmic membrane of the cable bacteria via the DsrMK and QmoABC membrane complexes, respectively (Fig. 3). This model is, to a large extent, a reversal of the electron flow during dissimilatory sulfate reduction (21, 28), and similar to the electron transport proposed for sulfide-oxidizing microorganisms utilizing the rDSR pathway (35). It is supported by the proteomic detection of QmoAB and DsrMK; only the membrane-bound subunit QmoC was not detected ([Dataset S2](#)). The lack of Dsr(J)OP ([SI Appendix, Fig. S3](#)) and other membrane complexes, which, in sulfate reducers, typically transport electrons between cytoplasm and periplasm, may indicate that cable bacteria tightly control the flow of electrons between cytoplasm and periplasm ([SI Appendix, SI Discussion](#)). In sulfate-reducing microorganisms, the QmoABC and DsrMK(JOP) complexes were proposed to facilitate energy conservation by generating a proton gradient across the cytoplasmic membrane (28, 37), although this has not been experimentally validated. This proton translocation is scalar and thus obtained by releasing protons from the oxidation of quinone on the periplasmic side of the cytoplasmic membrane. The QmoAC and DsrMK complexes of cable bacteria share high amino acid similarity and identical cytoplasmic membrane topology to those of sulfate-reducing members of the family Desulfobulbaceae. For this reason and because the complexes are inferred to reduce the quinone pool during S oxidation (Fig. 3), it is unlikely that they are directly involved in energy conservation in cable bacteria.

**Electron Transfer across the Membrane and in the Periplasm.** The proposed LDET by periplasmic fibers requires electrons to be passed from the quinone pool to the periplasm (Fig. 3). In *Geobacter*, such electron transfer is facilitated by one of at least 2 membrane-bound cytochrome *bc* complexes (ImcH, CbcL) that deliver electrons to soluble periplasmic cytochromes (38, 39), whereas, in *Shewanella*, this function is fulfilled by the multiheme cytochrome CymA (40–42). Homologs of ImcH, CbcL, and CymA are absent in cable bacteria, which, however, encode 2 structurally similar complexes that may enable electron transfer coupled to quinol oxidation (Fig. 3): a Rieske Fe-S domain protein with an adjacent membrane-bound cytochrome *b*-domain protein and an orphan homolog of the CydA subunit of the membrane-bound *bd* quinol oxidase ([SI Appendix, Fig. S4 and SI Discussion](#)). We speculate that quinol oxidation by these complexes results in a proton gradient across the membrane (Fig. 3 and [SI Appendix, SI Discussion](#)) and that they thus represent a key site for energy conservation in cable bacteria.

Soluble cytochromes may then act as electron shuttles in the periplasm, as described for multiheme cytochromes in *Geobacter* and *Shewanella* (40). With the exception of the diheme cytochrome MacA (43), which, in cable bacteria, is predicted as not membrane-associated, no homologs of those well-studied periplasmic cytochromes (e.g., Ppc, Fcc, STC) are present in cable bacteria. Instead, several multiheme cytochromes and 2 single-heme cytochromes with predicted periplasmic or extracytoplasmic localization are conserved among cable bacteria, and some were also expressed in *Ca. Electronema* sp. GS ([SI Appendix, Table S5 and Dataset S2](#)). Resonance Raman microscopy showed high abundance of c-type cytochromes in living cable bacteria (18), and these c-type cytochromes were most abundant in the cell envelope, as also revealed by Raman microscopy ([SI Appendix, Fig. S5](#)).

We therefore propose a model whereby periplasmic c-type cytochromes transfer electrons from the Rieske–cytochrome *b* complex or the CydA homolog to periplasmic fibers for LDET (Fig. 3). As shown for *Geobacter* (44), highly abundant c-type cytochromes could also act as capacitors in sulfide-oxidizing cells during short periods without access to oxygen.

**LDET: A Role for Periplasmic Cytochromes or Conductive Pili?** At present, the conductive structures enabling LDET in cable bacteria have not been identified (17), but fiber structures running in parallel through the joint periplasm of all cells have been designated as prime candidates (1, 20). Type IV pili (45) and, recently, multiheme cytochrome nanowires (46) have been described as electrically conductive fibers; could they be candidates for (part of) the conductive structure? The cytochrome nanowires of *Geobacter*, with a diameter of 4 nm and a length of a few nanometers, consist of polymerized hexaheme cytochromes (OmcS). Cable bacteria contain no OmcS homologs ([SI Appendix, Table S5](#)), but other c-type cytochromes are abundant in their cell envelope ([SI Appendix, Fig. S5](#)) and show a redox gradient along the cable bacterium filament (18). However, besides MacA, a cytochrome c554–hemoglobin fusion protein, and a cytochrome c554-containing putative nitrite reductase (all 3 of which are unlikely candidates for conductive fibers), only 2 single-heme cytochromes were detected in the proteome of *Ca. Electronema* sp. GS ([SI Appendix, Table S5 and Dataset S2](#)). Whether any of them would be conductive upon a possible polymerization (47) or form superstructures of larger diameters, possibly with other polymers (as discussed later), remains to be shown.

The electrically conductive pili (e-pili) of *Geobacter* and other, diverse bacteria (48, 49) consist of PilA with conserved aromatic amino acid residues. PilA was the single most abundant protein in the proteome of *Ca. Electronema* sp. GS (Fig. 2 and [Dataset S2](#)) and contained 4 of 5 aromatic residues conserved in the N-terminal part of PilA of *Geobacter sulfurreducens* and other bacteria (45, 48, 49) (Fig. 4). These aromatic residues seem to play a crucial role for the level of pilus-mediated electrical conduction in *G. sulfurreducens* and *Pseudomonas aeruginosa*, as shown by loss-of-function (50) and gain-of-function (51) experiments. Also, the overall densities of aromatic amino acids in PilA of cable bacteria (7 to 10%) are similar to that in experimentally confirmed e-pili (9 to 15% aromatic AAs) of diverse bacteria (49). Although the predicted cable bacteria PilA proteins show variation in length (59 to 182 aa; Fig. 4), length and electrical conductivity appear not to be correlated in e-pili (49). Type IV pili display a highly conserved N-terminal part with an alpha-helical structure forming the core of type IV pili polymers, and an extremely variable (in sequence and length) C-terminal part forming a beta strand-rich head domain (52). This head domain was recently suggested to form an insulating layer around the conductive core in type IV pili (53). The cable bacteria PilA feature the predicted alpha helix, conserved phenylalanine (F1), and glutamic acid (E5) of type IV pili, which are needed for prepilin cleavage, methylation, and pilin assembly (52–54), and the highly variable beta strand-rich head domain (Fig. 4). In contrast, cable bacteria PilA lack the random hook structure for metal interactions, including the exposed tyrosine (Y57), which is predicted to transfer electrons to solid electron acceptors (53, 54). Because of this predicted lack of metal interaction capability, the absence of external pili on the outside of cable bacteria filaments (1, 9, 19, 20), and the apparent lack of outer membrane cytochromes ([SI Appendix, Table S5](#)) to transfer electrons onto extracellular pili (55), we find it conceivable that PilA in cable bacteria does not form external e-pili but may assemble to internalized, periplasmic fibers.

Cable bacteria contain at least 2 operons of genes associated with type IV pili or type II secretion systems ([SI Appendix, Table](#)

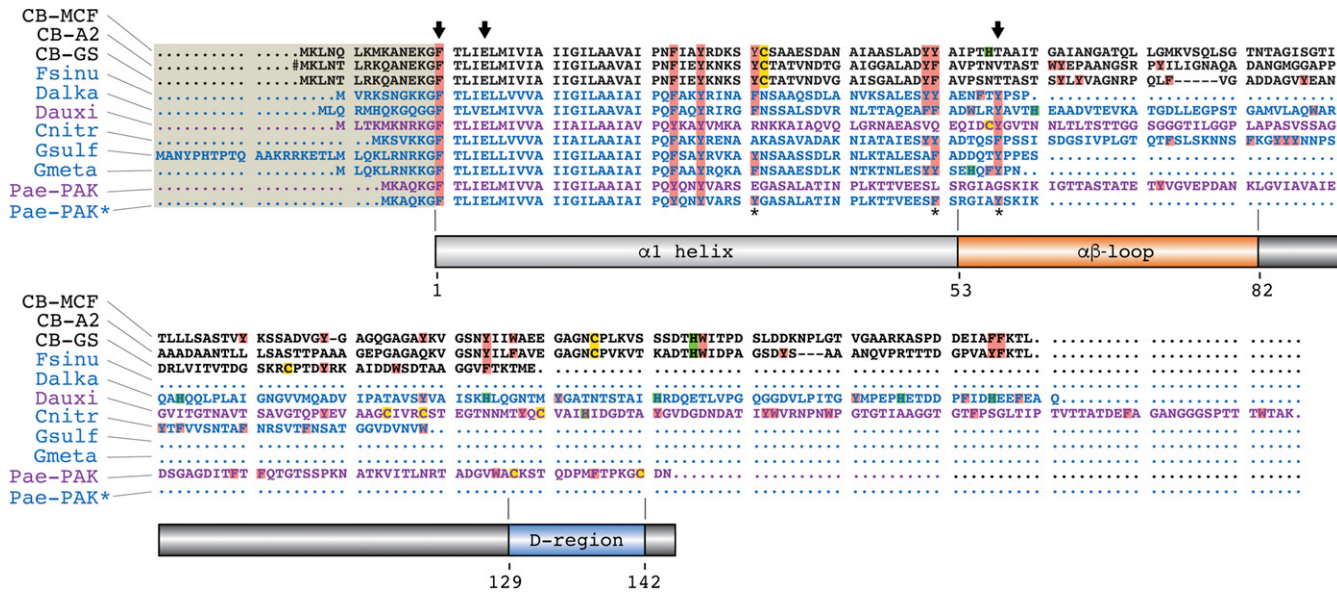


**Fig. 4.** Domain architecture and alignment of cable bacteria PilA amino acid sequences with PilA from experimentally confirmed e-pili (blue) of other bacteria (49), and with nonconductive PilA (purple) (49) for comparison. Pae-PAK\* shows a modified version of the Pae-PAK PilA, which was conductive upon truncation and insertion of 3 aromatic residues (asterisk) (51). Aromatic residues (red), histidines (green), and cysteines (yellow) are highlighted in the sequence; key residues mentioned in the text (F1, E5, Y57) are indicated with arrows. \*Manually corrected start site. CB\_A2, *Ca. Electrothrix marina* A2; CB\_GS, *Ca. Electronema* sp. GS; CB\_MCF, *Ca. Electrothrix aarhusiensis* MCF; Cnitr, *Calditerrivibrio nitroreducens*; Dalka, *D. alkaliphilus*; Dauxi, *Ca. Desulfoferoxidus auxilius*; Fsinu, *Flexistipes sinusarabici*; Gmeta, *Geobacter metallireducens*; Gsulf, *Geobacter sulfurreducens*; Pae-PAK, *P. aeruginosa*; Pae-PAK\*, *P. aeruginosa* modified PilA (51). Note that cable bacteria PilA do not contain a clear D-region, as only 1 cysteine is present in the distal C-terminal part of the head domain.

S6). However, the *pilA* genes in *Ca. E. aarhusiensis* MCF and *Ca. Electronema* sp. GS are not part of any of those operons but instead linked to genes encoding proteins with tetratricopeptide repeats (*SI Appendix*, Fig. S6). These repeats represent a structural motif mediating protein–protein interactions (56), and it is tempting to speculate that this aids in assembling individual PilA subunits into continuous fibers that span the entire cable bacterium filament. Ultrastructural analyses have shown a diameter of approximately 50 nm for the periplasmic fibers (20), whereas type IV pili have a diameter of 3 to 5 nm in *G. sulfurreducens* (45), and so would have to form larger superstructures or integrate with other polymer structures into larger assemblies (*SI Appendix*). Based on proteogenomic and imaging data, we therefore suggest that LDET in cable bacteria occurs in periplasmic fibers consisting of multiple e-pili or of carbohydrate backbones “decorated” with pilin (or possibly cytochromes). We emphasize, however, that this model is only a hypothesis that needs to be experimentally tested.

**Oxygen Reduction and Detoxification.** The last step in e-SOx is the transfer of electrons from the periplasmic fibers to the terminal electron acceptor, most commonly oxygen (Fig. 1A). Surprisingly, we were unable to identify terminal oxidases in any cable bacterium genome or in the proteome of *Ca. Electronema* (*SI Appendix*, Table S5 and Dataset S3), with a single exception: the single-filament genome of *Ca. Electrothrix communis* A1 possibly encodes a membrane-bound cytochrome *c* oxidase (*SI Appendix*, *SI Discussion*). Most delta-proteobacterial sulfate reducers carry the quinol-dependent, membrane-bound terminal oxidase CydAB (57). In contrast, cable bacteria contain only a homolog of the quinol oxidase subunit CydA (as detailed earlier; *SI Appendix*, *Discussion*), whereas the oxygen reductase subunit is absent.

In the absence of membrane-bound terminal oxidases, which could couple oxygen reduction to proton translocation and thus conserve energy in the oxygen-respiring cells, we hypothesize that cable bacteria reduce oxygen by periplasmic cytochromes without energy conservation. As discussed earlier, c-type cytochromes are conserved in cable bacteria genomes (*SI Appendix*,

*Table S5*), expressed in *Ca. Electronema* sp. GS (*Dataset S2*), abundant, and localized in the periplasm (*SI Appendix*, Fig. S5); they may also be involved in oxygen reduction, like in *Desulfovibrio* species, in which periplasmic oxygen reduction is correlated with c-type cytochrome activity (58). Alternatively, cable bacteria may utilize a unique, periplasmic fusion protein consisting of a cytochrome domain and 1 or 2 truncated hemoglobin domains (*SI Appendix*, Fig. S7A and B and *SI Discussion*). In mammalian cells, neuroglobin can act as electron donor for cytochrome *c* (59). In contrast, little is known about the function of hemoglobin in bacteria; suggested roles are nitrosative stress protection and oxygen sensing, binding, and activation (60–62). In *Bacillus subtilis*, a truncated hemoglobin efficiently binds and reduces oxygen to water (63). It is thus tempting to speculate that the unique fusion protein accepts electrons from the conducting fiber, with its 2 domains facilitating sensing, activation, and reduction of oxygen in the periplasm of cable bacteria (Fig. 3 and *SI Appendix*, Fig. S7). Besides the fusion protein, cable bacteria genomes also encode a truncated hemoglobin with a predicted periplasmic localization (*Dataset S2*), which could also serve a role in oxygen reduction (Fig. 3). Periplasmic oxygen reduction may lead directly to the production of water or, by 1-electron transfer, to reactive oxygen species (ROS) that immediately need to be detoxified to water (as detailed later).

Why may cable bacteria have abandoned membrane-bound terminal oxidases, and thus energy conservation, during LDET-fueled oxygen reduction? One explanation could be the high oxygen reduction rates required: in each filament, only a few cells are located in the oxic sediment surface, whereas many (often approximately 10 $\times$ ) more cells perform sulfide oxidation in the anoxic zone. To maintain electron balance, electron flow has to be at least 10 times higher in the oxic, cathodic cells than in the anoxic, anodic cells (2). This may explain why the estimated cell-specific oxygen reduction rates are 4 to 14 $\times$  higher in cable bacteria than in closely related sulfate reducers or in aerobic sulfide oxidizers (2). Thus, oxygen reduction may have been optimized for speed instead of energy conservation.

High cell-specific oxygen reduction rates usually result in high production of reactive oxygen species (64). Cable bacteria possess multiple systems for protection against oxidative stress, both periplasmic and cytoplasmic (Fig. 3, Dataset S3, and *SI Appendix, SI Discussion*). Several key enzymes, i.e., catalase, superoxide reductase, and rubrerythrin, were also detected in the proteome of *Ca. Electronema* sp. GS (Dataset S2). In addition, the chaperonins GroEL/ES and several general stress proteins are among the highest expressed proteins (Fig. 2 and Dataset S2 and S3); they may, as for other bacteria, e.g., *Escherichia coli* (65) or *Caulobacter crescentus* (66), also play a protective role during oxidative stress in cells exposed to oxygen.

**Nitrate and Nitrite as Alternative Electron Acceptors.** Geochemical and electrical potential measurements in marine sediment have shown that cable bacteria can couple anodic sulfide oxidation via LDET to the cathodic reduction of nitrate and nitrite, but not nitrous oxide (7, 67). This indicates that cable bacteria reduce nitrate and nitrite to NO, N<sub>2</sub>O, or ammonium. The cable bacteria genomes encode the periplasmic nitrate reductase NapAB (Dataset S3) but no typical nir- or nrf-type nitrite reductase (68). However, a periplasmic multiheme cytochrome (*SI Appendix, Table S5*) is encoded adjacent to the nap operon and was expressed in *Ca. Electronema* sp. GS (Dataset S2). The inferred protein shares 57% sequence identity with a homolog from an orange *Ca. Maribeggiatoa* sp. (locus tag BOGUAY\_0691), which reduced nitrite to ammonium in vitro (69). We therefore hypothesize that cable bacteria can couple sulfide oxidation with nitrate reduction to ammonium (Fig. 3), and suspect that one of the periplasmic cytochromes could transfer the electrons to the catalytic enzymes.

**Cable Bacteria Are Capable of Autotrophic CO<sub>2</sub> Fixation and Show Limited Organotrophic Potential.** A mixotrophic metabolism, i.e., inorganic sulfur as electron donor and an organic carbon source, has been inferred for cable bacteria based on geochemical data (11) and time-series experiments (2). Organic carbon assimilation has been experimentally confirmed for marine cable bacteria, which incorporated <sup>13</sup>C-propionate but not (or only to a minor extent) <sup>13</sup>C-bicarbonate (70). However, like other autotrophic members of the family Desulfobulbaceae (71, 72), cable bacteria encode the complete Wood-Ljungdahl pathway (*SI Appendix, Table S7*), and most of its proteins were detected in the proteome of *Ca. Electronema* sp. GS (*SI Appendix, Table S7* and Dataset S2). This pathway may facilitate CO<sub>2</sub> fixation to acetyl-CoA (73), which would require reducing power in the form of ferredoxin (*SI Appendix, SI Discussion*). In addition, a periplasmic carbonic anhydrase (CA) was expressed in *Ca. Electronema* sp. GS (Dataset S2); CAs are typically used by autotrophs to convert bicarbonate into CO<sub>2</sub> that freely diffuses over the membrane, enhancing CO<sub>2</sub> fixation (74). We experimentally confirmed <sup>14</sup>CO<sub>2</sub> uptake by cable bacteria enriched from Aarhus Bay using microautoradiography and fluorescence in situ hybridization (MAR-FISH; *SI Appendix, SI Methods*). Of 51 cable bacteria filaments analyzed, 43% showed incorporation of <sup>14</sup>C-bicarbonate (Fig. 5A and *SI Appendix, Fig. S8A*), and quantification of MAR-derived silver grains per micrometer revealed a 20-fold difference in <sup>14</sup>C-bicarbonate uptake between individual filaments (*SI Appendix, Fig. S8B*). These data provide evidence that cable bacteria can fix CO<sub>2</sub>, but the activity varied strongly. In addition, cable bacteria have the genetic potential to fix N<sub>2</sub> (*SI Appendix, SI Discussion* and Dataset S3). The quantitative importance and environmental regulation of autotrophy and diazotrophy compared with heterotrophy are currently unknown. When growing autotrophically, many sulfate reducers, including members of the family Desulfobulbaceae, use H<sub>2</sub> as electron donor (8, 75). In contrast, periplasmic hydrogenases are absent in cable bacteria, and only *Ca. E. aarhusiensis* MCF encodes a cy-

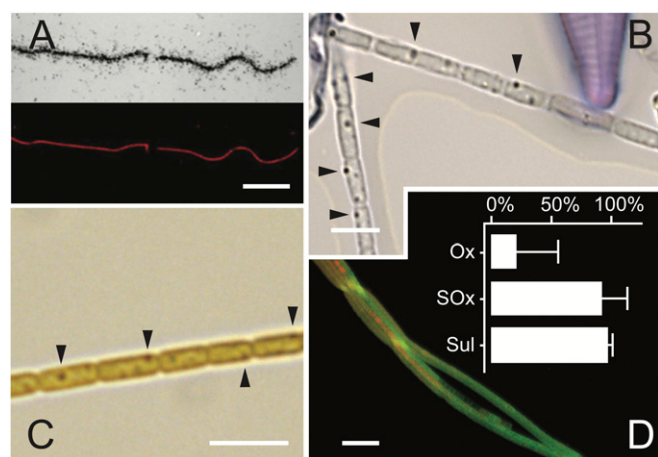


**Fig. 5.** Visualization of CO<sub>2</sub> assimilation, storage compounds, and protein biosynthesis in cable bacteria. (A) The <sup>14</sup>C-bicarbonate uptake detected by microautoradiography (MAR; black spots; *Upper*) of a single filament of *Ca. Electrothrix* spp. identified by fluorescence in situ hybridization (FISH; *Lower*). (Scale bar, 40  $\mu$ m.) (B) Polyphosphate granules (black arrows) in filaments of *Ca. Electrothrix* sp. GS. Polyphosphate inclusions (0 to 4 per cell) appear as dark spheres after staining with toluidine blue. (Scale bar, 5  $\mu$ m.) (C) Polyglucose granules (black arrows) in a single filament of *Ca. Electronema* sp. GS as detected by light microscopy after iodine staining. (Scale bar, 5  $\mu$ m.) (D) Active protein biosynthesis in several filaments of *Ca. Electrothrix* spp. detected by BONCAT (green) and overlaid with FISH identification of cable bacteria (red). (Scale bar, 20  $\mu$ m.) (Inset) Fraction of cable bacteria cells that were BONCAT-positive in the oxic (Ox), suboxic (SOx), and sulfidic (Sul) sediment layers, respectively. Bars and error bars represent mean values with SD;  $n = 11$  (Ox),  $n = 21$  (SOx), and  $n = 17$  (Sul) filaments; in total, more than 3,000 cells were analyzed.

toplasmic hydrogenase (*SI Appendix, SI Discussion*), suggesting that H<sub>2</sub> is not a general electron donor for cable bacteria.

Heterotrophic potential appears rather limited according to our genome analysis: formate may be assimilated via the Wood-Ljungdahl pathway (76), and acetate by the enzyme acetyl-CoA synthetase, both into acetyl-CoA as first intermediate; propionate assimilation, as observed in marine cable bacteria (70), may proceed via the methylmalonyl-CoA pathway to succinyl-CoA, similar to propionate degradation in *Desulfobulbus* species (77); all 4 enzymes catalyzing this pathway are encoded in the genome of *Ca. E. aarhusiensis* MCF (*SI Appendix, Table S8*). In contrast, *Ca. Electronema* sp. GS lacks the methylmalonyl-CoA pathway and the gene coding for succinyl-CoA synthetase, which would link into the TCA cycle; *Ca. Electronema* sp. GS should thus be incapable of assimilating propionate.

Generally, genes encoding amino acid and carbohydrate transport and catabolism are underrepresented in cable bacteria compared with other Desulfobulbaceae (*SI Appendix, Fig. S1*), indicating a limited potential for organic carbon assimilation and dissimilation.

Specifically, unlike most other members of the family Desulfobulbaceae, cable bacteria lack genes encoding lactate dehydrogenase and the beta-oxidation of fatty acids. We note, however, that acetate dissimilation could, in principle, proceed via the Wood-Ljungdahl pathway operating in oxidative direction, as known from acetate oxidation by sulfate reducers (78). Cable bacteria do also encode 4 different unspecific Fe and Zn alcohol dehydrogenases (matching pfam00465 and pfam00107), suggesting a potential for catabolizing alcohols (Dataset S3).

In many sulfate-reducing bacteria, as well as other anaerobes, growth on organic compounds is dependent on electron-bifurcating reactions involving heterodisulfide reductase (HdrABC) (21, 79). HdrABC is encoded in all *Desulfobulbus* genomes by the linked

*hdrABC* and also in the genome of *Ca. E. aarhusiensis* MCF. In contrast, *hdrB* is absent and *hdrA* and *hdrC* are not linked in *Ca. Electronema* sp. GS; both HdrA and HdrC were detected in the proteome and are possibly involved in CO<sub>2</sub> fixation and sulfur disproportionation, respectively, rather than organotrophic growth (*SI Appendix, SI Discussion*). This observation suggests a greater organotrophic potential for *Ca. E. aarhusiensis* MCF compared with *Ca. Electronema* sp. GS. In support of this, *Ca. E. aarhusiensis* MCF encodes a full TCA cycle, whereas *Ca. Electronema* sp. GS lacks several genes, including genes encoding the aforementioned key enzyme succinyl-CoA-synthase (*SI Appendix, Fig. S9*).

Cable bacteria encode a full glycolytic and Entner–Doudoroff pathway, except that all 6 genomes lack genes encoding the enzyme enolase (*SI Appendix, Fig. S9*). The absence of enolase, although unusual, has also been reported for *Butyrivibrio proteoclasticus* and Bacteroidetes family BS1 (80, 81), in which it is rescued by the methylglyoxal detoxification pathway. With its key enzyme, methylglyoxal synthase, missing in cable bacteria, we suspect them to contain a different, yet unknown, “work-around” to complete glycolysis.

**Storage Compounds.** Polyphosphate granules have been described in marine cable bacteria (15, 82), and many sulfate reducers can store poly-hydroxyalkanoates (PHAs) as carbon and energy reserves (83). Cable bacteria carry the genes for polyphosphate kinases (*ppk1* and *ppk2*; *Dataset S3*) and thus have the genetic potential to produce and use polyphosphates (Fig. 3); *Ppk1* was also detected in the proteome of *Ca. Electronema* sp. GS. These kinases catalyze the polymerization and depolymerization of polyphosphate by transfer of the terminal phosphate group of ATP or GTP or phosphorylation of ADP/AMP or GDP (84–86); therefore, polyphosphate could be an energy storage for cable bacteria. *Ca. E. aarhusiensis* MCF, but not *Ca. Electronema* sp. GS, also possesses an exopolyphosphatase, which catalyzes the terminal cleavage of polyphosphate, releasing P<sub>i</sub> (84). We confirmed the presence of polyphosphate granules in *Ca. Electronema* sp. GS by light microscopy and in cable bacteria filaments enriched from Aarhus Bay by electron microscopy (Fig. 5B and *SI Appendix, Fig. S11*).

No genes for the production or breakdown of PHA were detected in the cable bacteria genomes. However, cable bacteria have the genetic potential for the interconversion of polyglucose and glucose (*SI Appendix, Fig. S9* and *Dataset S3*) and thus may use polyglucose as carbon and energy storage (87, 88). In support of these predictions, polyglucose granules were detected in *Ca. Electronema* sp. GS (Fig. 5C). In addition to providing energy, polyglucose degradation could, as in sulfate reducers (75), fuel oxygen detoxification by providing NADH for the cytoplasmic rubredoxin-oxygen oxidoreductase (*SI Appendix, SI Discussion*).

**Motility and Chemotaxis.** Cable bacteria are motile and actively position themselves in an oxygen-sulfide gradient, presumably by chemotaxis (89). Cable bacteria genomes do not contain flagella genes, but instead several polysaccharide exporters, which could be involved in excretion-based gliding motility (*SI Appendix, SI Discussion*). This is also indicated by trails of extracellular polymeric substances (EPSs) left behind by cable bacteria on glass slides (82). Cable bacteria contain only 3 chemotaxis operons, compared with 11 to 23 in other Desulfobulbaceae (*SI Appendix, SI Discussion*), and a comparably low density of regulatory genes (*SI Appendix, Fig. S12*); this indicates a limited or highly focused response capability to environmental signals.

**Ecological Implications.** Collapses of cable bacteria populations have been observed in laboratory incubations (2, 3, 13) and field surveys (14, 90), and have been explained by resource depletion, most notably the depletion of the sedimentary iron-sulfide pool, which fuels anodic sulfide oxidation (17). Alternatively, cable

bacteria may, like other blooming organisms, experience a high rate of virus predation according to the “kill-the-winner” hypothesis (91); indeed, their genomes bear restriction-modification enzymes, toxin-antitoxin modules (*SI Appendix, Table S9*), and CRISPR regions (*SI Appendix, Table S10*) as evidence of previous virus attack (92–94) (*SI Appendix, SI Discussion*). Yet another factor limiting cable bacteria blooms may be the pronounced pH peak of 8.5 and higher produced by cable bacteria in the oxic sediment surface (1, 2, 95): isoelectric-point analysis of the periplasm (and thus external pH)-exposed proteins of cable bacteria suggests that they are adapted to neutral pH (*SI Appendix, Fig. S13*) and may become denatured under alkaline conditions; this may contribute to the collapse of cable bacteria blooms (*SI Appendix, SI Discussion*).

**A Conceptual Model for Metabolism and Lifestyle of Cable Bacteria.** Taken together, our data suggest that cable bacteria, even though, at first glance, their genomes resemble sulfate-reducing Desulfobulbaceae, are chemolithoautotrophs and mixotrophs that oxidize sulfide by reversing the canonical sulfate reduction pathway (Fig. 3). Electrons are channeled via the quinone pool into the periplasm, where cytochromes transfer them onto conductive fibers that contain e-pili. After LDET over centimeter distances, electrons are transferred directly from the periplasmic fibers to the terminal electron acceptors oxygen, nitrate, and nitrite, which are reduced by periplasmic enzymes, apparently without further energy conservation. This model implies that energy conservation occurs only in the anodic, sulfide-oxidizing cells, both by substrate-level and oxidative phosphorylation. In contrast, the cathodic, oxygen- or nitrate-reducing cells would have no means of energy conservation but merely act as electron sink for the entire cable bacterium filament. A first indication for this unusual division of labor is provided by visualizing active protein biosynthesis in marine cable bacteria from oxic, suboxic, and sulfidic sediment layers by bioorthogonal noncanonical amino acid tagging (BONCAT) (96). In agreement with the proposed energy distribution, >90% of cable bacteria cells detected in the suboxic and sulfidic layers were actively synthesizing new protein, whereas protein biosynthesis in the oxic surface cells could be detected in only very few filaments, accounting for approximately 20% of oxic cable bacteria cells (Fig. 5D).

The cable bacteria’s evolutionary descent from obligate anaerobic sulfate reducers implies that a lack of energy conservation is not their only challenge in the oxic zone: oxygen likely is inhibitory to many of their core enzymatic systems, high oxygen reduction rates inevitably generate abundant reactive oxygen species, and the high pH may inhibit and denature periplasmic and outer membrane proteins. Yet, for the multicellular cable bacterium, the lack of growth and a high death risk for the cells in the oxic zone may constitute an affordable price for access to a potent electron sink and the monopolization of sulfide oxidation. The chemotaxis of cable bacteria and their ability to move in loops (89) allows each filament to direct a few cells at a time to the oxic zone to fulfill their essential cathodic function, i.e., flaring off electrons by reducing oxygen. While exposed to oxygen, these cells may live on their storage compounds (polyphosphate and polyglucose; Fig. 5) that have been accumulated and can be recharged during periods in the anoxic zone.

In conclusion, our analyses provide a glimpse at how cable bacteria may work, using the genome fraction for which functions could be assigned. Many of the hypotheses outlined here, although generally well supported by gene homology, gene expression, and functional data, still need to be proven experimentally. Last but not least, a large fraction of the genomes remains uncharacterized; in particular, the limited number of unique, conserved, hypothetical proteins, which were detected in the proteome (*Datasets S1* and *S2*), are prime candidates for

future studies, and may support or challenge the current metabolic model for cable bacteria.

## Materials and Methods

*SI Appendix* includes a detailed description of the study materials and methods.

**Genome Sequencing.** The 5 *Ca. Electrothrix* draft genomes were generated from 6 single filaments, which were extracted by micromanipulation with capillary glass hooks from whole sediment cores enriched for cable bacteria as previously described (1). Whole genomes were amplified from individual filaments using the GenomePlex Single Cell Whole Genome Amplification Kit (Sigma-Aldrich). The amplified DNA was sequenced on an Ion Torrent PGM sequencer (Life Technologies). The *Ca. Electronema* sp. GS draft genome was assembled from a low-complexity metagenome obtained from a cable bacterium enrichment culture by sequencing of extracted DNA on an Illumina MiSeq system.

**Genome Reconstruction and Annotation.** The individual sequence libraries were assembled with gsAssembler version 2.6 (Roche 454 Life Sciences) and SPAdes version 2.2.1 (97); assembly refinement procedures, quality checks, and further genome analyses are described in detail in *SI Appendix, Methods*. The resultant cable bacteria draft genomes were annotated using the IMG-ER pipeline (98).

**Proteome Analysis.** A metaproteome was generated from 500 µL sediment of the *Ca. Electronema* sp. GS enrichment culture. Proteins were extracted, separated by SDS/PAGE, analyzed by mass spectrometry, and identified by comparison against the annotated *Ca. Electronema* sp. GS draft genome (*SI Appendix, Methods*).

**Raman Microspectroscopy.** C-type cytochromes were detected in individual cable bacteria cells on a confocal Raman microscope (Horiba) as described previously (18). For each cell, 2 to 3 line scans with 10 to 20 measuring points each were performed across the filament. The largest cytochrome peak ( $\nu$ 15 mode at  $750\text{ cm}^{-1}$ ) was used for a relative quantification of cytochromes across the cable bacterium filament.

1. C. Pfeffer et al., Filamentous bacteria transport electrons over centimetre distances. *Nature* **491**, 218–221 (2012).
2. R. Schauer et al., Succession of cable bacteria and electric currents in marine sediment. *ISME J.* **8**, 1314–1322 (2014).
3. S. Y. Malkin et al., Natural occurrence of microbial sulphur oxidation by long-range electron transport in the seafloor. *ISME J.* **8**, 1843–1854 (2014).
4. N. Risgaard-Petersen et al., Cable bacteria in freshwater sediments. *Appl. Environ. Microbiol.* **81**, 6003–6011 (2015).
5. L. D. W. Burdorf et al., Long-distance electron transport occurs globally in marine sediments. *Biogeosciences* **14**, 683–701 (2017).
6. L. P. Nielsen, N. Risgaard-Petersen, H. Fossing, P. B. Christensen, M. Sayama, Electric currents couple spatially separated biogeochemical processes in marine sediment. *Nature* **463**, 1071–1074 (2010).
7. U. Marzocchi et al., Electric coupling between distant nitrate reduction and sulfide oxidation in marine sediment. *ISME J.* **8**, 1682–1690 (2014).
8. J. Kuever, “The family Desulfobulbaceae” in *The Prokaryotes*, E. Rosenberg, E. F. DeLong, S. Lory, E. Stackebrandt, F. Thompson, Eds. (Springer, Heidelberg, 2014), pp. 75–86.
9. D. Trojan et al., A taxonomic framework for cable bacteria and proposal of the candidate genera *Electrothrix* and *Electronema*. *Syst. Appl. Microbiol.* **39**, 297–306 (2016).
10. J. Klier, O. Dellwig, T. Leipe, K. Jürgens, D. P. R. Herlemann, Benthic bacterial community composition in the oligohaline-marine transition of surface sediments in the Baltic Sea based on rRNA analysis. *Front. Microbiol.* **9**, 236 (2018).
11. N. Risgaard-Petersen, A. Revil, P. Meister, L. P. Nielsen, Sulfur, iron-, and calcium cycling associated with natural electric currents running through marine sediment. *Geochim. Cosmochim. Acta* **92**, 1–13 (2012).
12. F. J. R. Meysman, N. Risgaard-Petersen, S. Y. Malkin, L. P. Nielsen, The geochemical fingerprint of microbial long-distance electron transport in the seafloor. *Geochim. Cosmochim. Acta* **152**, 122–142 (2015).
13. A. M. F. Rao, S. Y. Malkin, S. Hidalgo-Martinez, F. J. R. Meysman, The impact of electrogenic sulfide oxidation on elemental cycling and solute fluxes in coastal sediment. *Geochim. Cosmochim. Acta* **172**, 265–286 (2016).
14. D. Seitaj et al., Cable bacteria generate a firewall against euxinia in seasonally hypoxic basins. *Proc. Natl. Acad. Sci. U.S.A.* **112**, 13278–13283 (2015).
15. F. Sulu-Gambari et al., Impact of cable bacteria on sedimentary iron and manganese dynamics in a seasonally-hypoxic marine basin. *Geochim. Cosmochim. Acta* **192**, 49–69 (2016).
16. A. J. Kessler et al., Cable bacteria promote DNRA through iron sulfide dissolution. *Limnol. Oceanogr.* **64**, 1228–1238 (2019).
17. F. J. R. Meysman, Cable bacteria take a new breath using long-distance electricity. *Trends Microbiol.* **26**, 411–422 (2018).
18. J. T. Bjerg et al., Long-distance electron transport in individual, living cable bacteria. *Proc. Natl. Acad. Sci. U.S.A.* **115**, 5786–5791 (2018).
19. Z. Jiang et al., In vitro single-cell dissection revealing the interior structure of cable bacteria. *Proc. Natl. Acad. Sci. U.S.A.* **115**, 8517–8522 (2018).
20. R. Cornelissen et al., The cell envelope structure of cable bacteria. *Front. Microbiol.* **9**, 3044 (2018).
21. I. A. C. Pereira et al., A comparative genomic analysis of energy metabolism in sulfate reducing bacteria and archaea. *Front. Microbiol.* **2**, 69 (2011).
22. J. F. Imhoff, “The family Ectothiorhodospiraceae” in *The Prokaryotes*, M. Dworkin, S. Falkow, E. Rosenberg, K.-H. Schleifer, E. Stackebrandt, Eds. (Springer, Heidelberg, 2006), pp. 874–886.
23. H. N. Schulz, “The genus *Thiomargarita*” in *The Prokaryotes*, M. Dworkin, S. Falkow, E. Rosenberg, K.-H. Schleifer, E. Stackebrandt, Eds. (Springer, Heidelberg, 2006), pp. 1156–1163.
24. A. Teske, D. C. Nelson, “The genera *Beggiatoa* and *Thioploca*” in *The Prokaryotes*, M. Dworkin, S. Falkow, E. Rosenberg, K.-H. Schleifer, E. Stackebrandt, Eds. (Springer New York, 2006), pp. 784–810.
25. H. Müller et al., Long-distance electron transfer by cable bacteria in aquifer sediments. *ISME J.* **10**, 2010–2019 (2016).
26. L. M. Chailakhyan et al., Intercellular power transmission along trichomes of cyanobacteria. *Biochim. Biophys. Acta* **679**, 60–67 (1982).
27. C. Dahl, C. G. Friedrich, Eds, *Microbial Sulfur Metabolism* (Springer, New York, 2008).
28. A. A. Santos et al., A protein trisulfide couples dissimilatory sulfate reduction to energy conservation. *Science* **350**, 1541–1545 (2015).
29. C. Thorup, A. Schramm, A. J. Findlay, K. W. Finster, L. Schreiber, Disguised as a sulfate reducer: Growth of the delta-proteobacterium *Desulfurivibrio alkophilus* by sulfide oxidation with nitrate. *MBio* **8**, 1–9 (2017).
30. A. Pellerin et al., Large sulfur isotope fractionation by bacterial sulfide oxidation. *Sci. Adv.* **5**, eaaw1480 (2019).
31. K. Fuseler, D. Krekeler, U. Sydow, H. Cypionka, A common pathway of sulfide oxidation by sulfate-reducing bacteria. *FEMS Microbiol. Lett.* **144**, 129–134 (1996).
32. M. Jormakka et al., Molecular mechanism of energy conservation in polysulfide respiration. *Nat. Struct. Mol. Biol.* **15**, 730–737 (2008).
33. T. Koch, C. Dahl, A novel bacterial sulfur oxidation pathway provides a new link between the cycles of organic and inorganic sulfur compounds. *ISME J.* **12**, 2479–2491 (2018).

**Microautoradiography/FISH.** The ability of cable bacteria to assimilate dissolved inorganic carbon was analyzed by MAR-FISH. Marine cable bacteria enrichments were incubated with  $10\text{ }\mu\text{Ci mL}^{-1}$   $^{14}\text{C}$ -bicarbonate for 8 h at 15 °C. Cable bacteria were then fixed and immobilized, and MAR-FISH, imaging, and quantification of silver grains was done as previously described (99). Further details are provided in *SI Appendix, Methods*.

**Visualization of Polyphosphate and Polyglucose Inclusions in Cable Bacteria.** Polyphosphate granules were visualized by light microscopy after toluidine blue staining (100) and by transmission electron microscopy (TEM) on a Tecnai Spirit microscope (120 kV); polyphosphate was confirmed by scanning electron microscopy (SEM) on a NanoSEM (Nova 600; FEI) operated at low vacuum and low voltage (3 kV) with an integrated energy dispersive X-ray spectrometer (EDX) with 20 keV beam energy. Cable bacteria were hand-picked, transferred onto EM grids, and dried at room temperature. Polyglucose was visualized by light microscopy after iodide staining (100).

**Bioorthogonal Noncanonical Amino Acid Tagging (BONCAT).** Active protein biosynthesis in cable bacteria filaments was visualized by BONCAT (96). Marine sediment cores enriched for cable bacteria were incubated with  $500\text{ }\mu\text{M}$  L-homopropargylglycine (HPG) and sectioned into oxic, suboxic, and sulfidic layers as determined by microsensor measurements. BONCAT analysis and FISH identification of cable filaments were performed from each layer (*SI Appendix, Methods*).

**ACKNOWLEDGMENTS.** We thank Lars B. Pedersen for sediment collection; Britta Poulsen, Susanne Nielsen, Trine Bech Søgaard, and Anne Stentebjerg for molecular lab assistance and genome sequencing; Heidi Vogt-Schulz for supporting the BONCAT analyses and insisting on the polyglucose staining; Krutika Bavishi for help with the cytochrome annotation; Gemma Reguera for insights on pilus structure; and the PRoteomics IDEntifications (PRIDE) team for support with proteomics data submission. This study was supported by the European Research Council (Advanced Grant 291650 to L.P.N. and Starting Grant 306933 to F.J.R.M.), the Danish National Research Foundation (DNRF104 and DNRF136), the Research Foundation Flanders (FWO project grant G031416N to F.J.R.M.), the Netherlands Organisation for Scientific Research (Vici Grant 016.VIDI.170.072 to F.J.R.M.), and the Danish Council for Independent Research | Natural Sciences & Technology and Production Sciences.

34. S. S. Venceslau, Y. Stockdreher, C. Dahl, I. A. Pereira, The “bacterial heterodisulfide” DsrC is a key protein in dissimilatory sulfur metabolism. *Biochim. Biophys. Acta* **1837**, 1148–1164 (2014).
35. C. Dahl, “Sulfur metabolism in phototrophic bacteria” in *Modern Topics in the Phototrophic Prokaryotes: Metabolism, Bioenergetics, and Omics*, P. C. Hallenbeck, Ed. (Springer, Cham, 2017), pp. 27–66.
36. A. Marietou, H. Roy, B. B. Jorgensen, K. U. Kjeldsen, Sulfate transporters in dissimilatory sulfate reducing microorganisms: A comparative genomics analysis. *Front. Microbiol.* **9**, 309 (2018).
37. A. R. Ramos, K. L. Keller, J. D. Wall, I. A. Pereira, The membrane QmoABC complex interacts directly with the dissimilatory adenosine 5'-phosphosulfate reductase in sulfate-reducing bacteria. *Front. Microbiol.* **3**, 137 (2012).
38. J. E. Butler, N. D. Young, D. R. Lovley, Evolution of electron transfer out of the cell: Comparative genomics of six *Geobacter* genomes. *BMC Genomics* **11**, 40 (2010).
39. L. Zacharoff, C. H. Chan, D. R. Bond, Reduction of low potential electron acceptors requires the CbcL inner membrane cytochrome of *Geobacter sulfurreducens*. *Bioelectrochemistry* **107**, 7–13 (2016).
40. L. Shi, T. C. Squier, J. M. Zachara, J. K. Fredrickson, Respiration of metal (hydr)oxides by Shewanella and Geobacter: A key role for multihaem c-type cytochromes. *Mol. Microbiol.* **65**, 12–20 (2007).
41. T. A. Clarke et al., Structure of a bacterial cell surface decaheme electron conduit. *Proc. Natl. Acad. Sci. U.S.A.* **108**, 9384–9389 (2011).
42. Y. Zhong, L. Shi, Genomic analyses of the quinol oxidases and/or quinone reductases involved in bacterial extracellular electron transfer. *Front. Microbiol.* **9**, 3029 (2018).
43. J. M. Dantas, A. Brausemann, O. Einsle, C. A. Salgueiro, NMR studies of the interaction between inner membrane-associated and periplasmic cytochromes from *Geobacter sulfurreducens*. *FEBS Lett.* **591**, 1657–1666 (2017).
44. A. Esteve-Núñez, J. Sosnik, P. Visconti, D. R. Lovley, Fluorescent properties of c-type cytochromes reveal their potential role as an extracytoplasmic electron sink in *Geobacter sulfurreducens*. *Environ. Microbiol.* **10**, 497–505 (2008).
45. G. Reguera et al., Extracellular electron transfer via microbial nanowires. *Nature* **435**, 1098–1101 (2005).
46. F. Wang et al., Structure of microbial nanowires reveals stacked hemes that transport electrons over micrometers. *Cell* **177**, 361–369.e10 (2019).
47. S. Hirota et al., Cytochrome c polymerization by successive domain swapping at the C-terminal helix. *Proc. Natl. Acad. Sci. U.S.A.* **107**, 12854–12859 (2010).
48. D. E. Holmes, Y. Tang, D. J. F. Walker, D. R. Lovley, The electrically conductive pili of *Geobacter* species are a recently evolved feature for extracellular electron transfer. *Microb. Genom.* **2**, e000072 (2016).
49. D. J. Walker et al., Electrically conductive pili from pilin genes of phylogenetically diverse microorganisms. *ISME J.* **12**, 48–58 (2018).
50. M. Vargas et al., Aromatic amino acids required for pilus conductivity and long-range extracellular electron transport in *Geobacter sulfurreducens*. *MBio* **4**, e00105–13 (2013). Erratum in: *MBio* **4**, e00210–13 (2013).
51. X. Liu et al., Biological synthesis of high-conductive pili in aerobic bacterium *Pseudomonas aeruginosa*. *Appl. Microbiol. Biotechnol.* **103**, 1535–1544 (2019).
52. L. Craig et al., Type IV pilus structure by cryo-electron microscopy and crystallography: Implications for pilus assembly and functions. *Mol. Cell* **23**, 651–662 (2006).
53. G. Reguera, Harnessing the power of microbial nanowires. *Microb. Biotechnol.* **11**, 979–994 (2018).
54. G. T. Feliciano, R. J. Steidl, G. Reguera, Structural and functional insights into the conductive pili of *Geobacter sulfurreducens* revealed in molecular dynamics simulations. *Phys. Chem. Chem. Phys.* **17**, 22217–22226 (2015).
55. T. Mehta, M. V. Coppi, S. E. Childers, D. R. Lovley, Outer membrane c-type cytochromes required for Fe(III) and Mn(IV) oxide reduction in *Geobacter sulfurreducens*. *Appl. Environ. Microbiol.* **71**, 8634–8641 (2005).
56. G. L. Blatch, M. Lässle, The tetratricopeptide repeat: A structural motif mediating protein-protein interactions. *Bioessays* **21**, 932–939 (1999).
57. R. S. Lemos et al., The ‘strict’ anaerobe *Desulfovibrio gigas* contains a membrane-bound oxygen-reducing respiratory chain. *FEBS Lett.* **496**, 40–43 (2001).
58. A. Baumgarten, I. Redenius, J. Kranczoch, H. Cypionka, Periplasmic oxygen reduction by *Desulfovibrio* species. *Arch. Microbiol.* **176**, 306–309 (2001).
59. A. Fago, A. J. Mathews, L. Moens, S. Dewilde, T. Brittain, The reaction of neuroglobin with potential redox protein partners cytochrome b5 and cytochrome c. *FEBS Lett.* **580**, 4884–4888 (2006).
60. S. N. Vinogradov, L. Moens, Diversity of globin function: Enzymatic, transport, storage, and sensing. *J. Biol. Chem.* **283**, 8773–8777 (2008).
61. M. D. Hade, J. Kaur, P. K. Chakraborti, K. L. Dikshit, Multidomain truncated hemoglobins: New members of the globin family exhibiting tandem repeats of globin units and domain fusion. *IUBMB Life* **69**, 479–488 (2017).
62. A. Bonamore et al., A novel chimera: The “truncated hemoglobin-antibiotic monooxygenase” from *Streptomyces avermitilis*. *Gene* **398**, 52–61 (2007).
63. E. Fernandez et al., Electron transfer reactions, cyanide and O<sub>2</sub> binding of truncated hemoglobin from *Bacillus subtilis*. *Electrochim. Acta* **110**, 86–93 (2013).
64. J. F. Turrens, B. A. Freeman, J. G. Levitt, J. D. Crapo, The effect of hyperoxia on superoxide production by lung submitochondrial particles. *Arch. Biochem. Biophys.* **217**, 401–410 (1982).
65. G. J. Hunter, T. Hunter, GroESL protects superoxide dismutase (SOD)-deficient cells against oxidative stress and is a chaperone for SOD. *Health* **5**, 1719–1729 (2013).
66. M. F. Susin, R. L. Baldini, F. Gueiros-Filho, S. L. Gomes, GroES/GroEL and DnaK/DnaJ have distinct roles in stress responses and during cell cycle progression in Caulobacter crescentus. *J. Bacteriol.* **188**, 8044–8053 (2006).
67. N. Risgaard-Petersen, L. R. Damgaard, A. Revil, L. P. Nielsen, Mapping electron sources and sinks in a marine biogeobattery. *J. Geophys. Res. G Biogeosciences* **119**, 1475–1486 (2014).
68. J. Simon, M. G. Klotz, Diversity and evolution of bioenergetic systems involved in microbial nitrogen compound transformations. *Biochim. Biophys. Acta* **1827**, 114–135 (2013).
69. B. J. MacGregor et al., Why orange Guaymas basin *Beggiatoa* spp. are orange: Single-filament-genome-enabled identification of an abundant octaheme cytochrome with hydroxylamine oxidase, hydrazine oxidase, and nitrite reductase activities. *Appl. Environ. Microbiol.* **79**, 1183–1190 (2013).
70. D. Vasquez-Cardenas et al., Microbial carbon metabolism associated with electrogenic sulphur oxidation in coastal sediments. *ISME J.* **9**, 1966–1978 (2015).
71. K. W. Finster et al., Complete genome sequence of *Desulfocapsa sulfexigens*, a marine delta-proteobacterium specialized in disproportionating inorganic sulfur compounds. *Stand. Genomic Sci.* **8**, 58–68 (2013).
72. E. D. Melton et al., Complete genome sequence of *Desulfurivibrio alkaliphilus* strain AHT2(T), a haloalkaliphilic sulfidogen from Egyptian hypersaline alkaline lakes. *Stand. Genomic Sci.* **11**, 67 (2016).
73. S. W. Ragsdale, E. Pierce, Acetogenesis and the Wood-Ljungdahl pathway of CO(2) fixation. *Biochim. Biophys. Acta* **1784**, 1873–1898 (2008).
74. E. Kupriyanova, N. Pronina, D. Los, Carbonic anhydrase—A universal enzyme of the carbon-based life. *Photosynthetica* **55**, 3–19 (2017).
75. R. Rabus et al., A post-genomic view of the ecophysiology, catabolism and technological relevance of sulphate-reducing prokaryotes. *Adv. Microb. Physiol.* **66**, 55–321 (2015).
76. K. Jansen, R. K. Thauer, F. Widdel, G. Fuchs, Carbon assimilation pathways in sulfate reducing bacteria. Formate, carbon dioxide, carbon monoxide, and acetate assimilation by *Desulfovibrio baarsii*. *Arch. Microbiol.* **138**, 257–262 (1984).
77. D. R. Kremer, T. A. Hansen, Pathway of propionate degradation in *Desulfovibulus propionicus*. *FEMS Microbiol. Lett.* **49**, 273–277 (1988).
78. R. K. Thauer, D. Möller-Zinkhan, A. M. Spormann, Biochemistry of acetate catabolism in anaerobic chemotrophic bacteria. *Annu. Rev. Microbiol.* **43**, 43–67 (1989).
79. A. R. Ramos et al., The FlxABCD-HdrABC proteins correspond to a novel NADH dehydrogenase/heterodisulfide reductase widespread in anaerobic bacteria and involved in ethanol metabolism in *Desulfovibrio vulgaris* Hildenborough. *Environ. Microbiol.* **17**, 2288–2305 (2015).
80. W. J. Kelly et al., The glycome of the rumen bacterium *Butyrivibrio proteoclasticus* B316(T) highlights adaptation to a polysaccharide-rich environment. *PLoS One* **5**, e11942 (2010).
81. L. M. Solden et al., New roles in hemicellulosic sugar fermentation for the uncultivated Bacteroidetes family BS11. *ISME J.* **11**, 691–703 (2017).
82. N. M. J. Geerlings, E. Zetsche, S. H. Martinez, J. J. Middelburg, F. J. R. Meysman, Mineral formation induced by cable bacteria performing long-distance electron transport in marine sediments. *Biogeosciences* **16**, 811–829 (2019).
83. T. Hai, D. Lange, R. Rabus, A. Steinbüchel, Polyhydroxyalcanoate (PHA) accumulation in sulfate-reducing bacteria and identification of a class III PHA synthase (PhaEC) in *Desulfovoccus multivorans*. *Appl. Environ. Microbiol.* **70**, 4440–4448 (2004).
84. A. Kornberg, N. N. Rao, D. Ault-Riché, Inorganic polyphosphate: A molecule of many functions. *Annu. Rev. Biochem.* **68**, 89–125 (1999).
85. L. Wang et al., Distribution patterns of polyphosphate metabolism pathway and its relationships with bacterial durability and virulence. *Front. Microbiol.* **9**, 782 (2018).
86. B. Nocek et al., Polyphosphate-dependent synthesis of ATP and ADP by the family-2 polyphosphate kinases in bacteria. *Proc. Natl. Acad. Sci. U.S.A.* **105**, 17730–17735 (2008).
87. P. Fareleira, J. Legall, A. V. Xavier, H. Santos, Pathways for utilization of carbon reserves in *Desulfovibrio gigas* under fermentative and respiratory conditions. *J. Bacteriol.* **179**, 3972–3980 (1997).
88. J. Preiss, Bacterial glycogen synthesis and its regulation. *Annu. Rev. Microbiol.* **38**, 419–458 (1984).
89. J. T. Bjerg, L. R. Damgaard, S. A. Holm, A. Schramm, L. P. Nielsen, Motility of electric cable bacteria. *Appl. Environ. Microbiol.* **82**, 3816–3821 (2016).
90. S. van de Velde et al., The impact of electrogenic sulfur oxidation on the biogeochemistry of coastal sediments: A field study. *Geochim. Cosmochim. Acta* **194**, 211–232 (2016).
91. T. F. Thingstad, Elements of a theory for the mechanisms controlling abundance, diversity, and biogeochemical role of lytic bacterial viruses in aquatic systems. *Limnol. Oceanogr.* **45**, 1320–1328 (2000).
92. W. A. M. Loenen, D. T. F. Dryden, E. A. Raleigh, G. G. Wilson, Type I restriction enzymes and their relatives. *Nucleic Acids Res.* **42**, 20–44 (2014).
93. H. Sberro et al., Discovery of functional toxin/antitoxin systems in bacteria by shotgun cloning. *Mol. Cell* **50**, 136–148 (2013).
94. J. Iranzo, A. E. Lobkovsky, Y. I. Wolf, E. V. Koonin, Evolutionary dynamics of the prokaryotic adaptive immunity system CRISPR-Cas in an explicit ecological context. *J. Bacteriol.* **195**, 3834–3844 (2013).
95. L. P. Nielsen, N. Risgaard-Petersen, Rethinking sediment biogeochemistry after the discovery of electric currents. *Annu. Rev. Mar. Sci.* **7**, 425–442 (2015).
96. R. Hatzendorf et al., In situ visualization of newly synthesized proteins in environmental microbes using amino acid tagging and click chemistry. *Environ. Microbiol.* **16**, 2568–2590 (2014).
97. A. Bankevich et al., SPAdes: A new genome assembly algorithm and its applications to single-cell sequencing. *J. Comput. Biol.* **19**, 455–477 (2012).
98. V. M. Markowitz et al., IMG: The integrated microbial genomes database and comparative analysis system. *Nucleic Acids Res.* **40**, D115–D122 (2012).
99. M. Nierychlo, J. L. Nielsen, P. H. Nielsen, “Studies of the ecophysiology of single cells in microbial communities by (Quantitative) microautoradiography and fluorescence in situ hybridization (MAR-FISH)” in *Hydrocarbon and Lipid Microbiology Protocols*, T. J. McGenity, K. N. Timmis, B. Nogales, Eds. (Springer, Berlin, Heidelberg, 2015), pp. 115–130.
100. H. N. Schulz, H. D. Schulz, Large sulfur bacteria and the formation of phosphorite. *Science* **307**, 416–418 (2005).